

Rapid 3D printing of unlayered, tough epoxy-alcohol resins with late gel points via dual-color curing technology

Supplementary Information

Florian Mayer,^a Dominik Laa,^b Thomas Koch,^b Jürgen Stampfl,^b Robert Liska,^a and Katharina Ehrmann^{a,*}

^{a.} *Institute of Applied Synthetic Chemistry, Technische Universität Wien, Vienna, Austria*

^{b.} *Institute of Materials Science and Technology, Technische Universität Wien, Vienna, Austria*

* Corresponding Author: katharina.ehrmann@tuwien.ac.at

Table of content

1.	Experimental.....	S2
2.	Macro-methacrylate analysis	S4
3.	Chain transfer mechanism for epoxides with alcohols.....	S5
4.	Epoxide screening.....	S6
5.	(Thermo)mechanical data of resorcinol diglycidylether-based IPNs with and without alcohols.	S7
6.	Photo-DSC results	S9
7.	DMTA results	S10
8.	3D printing of RT.....	S11
9.	3D printing of IPN 35 wt%	S12
10.	3D printing of IPN 50 wt%	S12
11.	References.....	S13

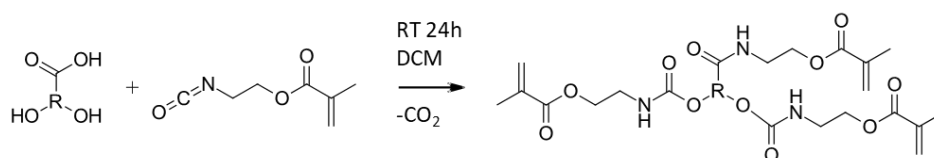
1. Experimental

Preparation and curing of epoxide-alcohol mixtures

The epoxide alcohol formulations were prepared by mixing and dissolving the monomers resorcinol diglycidylether (R) together with either cyclohexane dimethanol (C) or benzene dimethanol (B) or trimethylol propane (T) in equimolar ratios with respect to their reactive groups at 110 °C for one hour (Table S1). Afterwards, the mixtures were vortexed for at least 1 min to ensure homogeneity. The initiator UVI6976 (cationic photoinitiator containing a mixture of triarylsulfonium hexafluoroantimonate salts from DOW) was added to the homogeneous mixture and another heating step at 110 °C was applied for one hour to again dissolve all components and enable easy mixing of the components. The final formulation was vortexed once more for 1 min. Formulation curing was performed by distributing the liquid formulation into silicone moulds and curing at 100% intensity of the UV/vis-oven for 300 s per side (Uvitron International INTELLIRAY 600 UV-oven; 320-500 nm Hg broadband UV lamp; 600 W; UV-A: 125 mW cm⁻²; vis: 125 mW cm⁻²). The samples were post-cured in the dark at 110 °C for approximately 16 h. Samples that are cured this way will be referred to as “cationic single curing, ‘cs’” in the manuscript.

Polyester endgroup modification

The alcohol endgroups of the commercially available polyester Dynapol L208 (Evonic) were transformed into methacrylic end groups by mixing the polyester (9.854 g, 2.1 mmol) with dimethylaminopyridine (0.052 g, 0.4 mmol) in 80 mL dichloromethane, cooling the reaction mixture to 0 °C and adding 2-isocynoethyl methacrylate (0.654 g, 4.2 mmol) dropwise. After 30 min, the reaction mixture was allowed to warm up to room temperature and the reaction was proceeded for another 24 h. The product was precipitated in cold petroleum ether. For endgroup analysis the non-reacted residual OH-groups of the polyester were modified with 2-chloro-4,4,5,5-tetramethyl-1,3,2-dioxaphospholane and quantitative ³¹P-NMR was measured before and after modification (Figure S1, Figure S2). From the comparison with the unmodified polyester, a conversion of > 99% could be confirmed.



SchemeS1: Reaction scheme of the polyester modification. RT – room temperature, DCM – dichloromethane.

Preparation and curing of IPNs

The preparation of the IPN formulations was the same as for the epoxide-alcohol mixtures (Table S2). The curing step was performed in two steps. First, the soft network was cured in a Lumamat 100 light oven (400-500 nm, 6 Osram Dulux L Blue 18 W lamps) for 10 min per side. Samples that are at this stage will be referred to as “radical single curing, ‘rs’” in the manuscript. The second curing step was the same as for the hard network at 100% power of the UV/vis-oven for 300 s per side (Uvitron International INTELLIRAY 600 UV-oven; 320-500 nm Hg broadband UV lamp; 600 W; UV-A: 125 mW cm⁻²; vis: 125 mW cm⁻²). Afterwards the samples were post-cured at 110 °C in the dark for approximately 16 h. Samples that are at this stage will be referred to as “double cured ‘d’” in the manuscript.

³¹P-NMR for OH-number determination

Approximately 30 g of polyester (modified or unmodified) were dissolved in 0.3 mL of CDCl₃. 50 μL of a pyridine solution with 40 mg mL⁻¹ of cyclohexanol and 5 mg mL⁻¹ were added to this polyester solution. Separately, 50 μL of 2-chloro-4,4,5,5-tetramethyl-1,3,2-dioxaphospholane were mixed with 0.3 mL of CDCl₃ and added to the polyester solution. For this resulting solution, the ³¹P-NMR spectrum was measured. The integral of cyclohexanol (144.99 ppm) was set to one. At 147.30 ppm the aliphatic OH-groups of unmodified polyester could be integrated, while the acidic OH-groups of unmodified polyester could be integrated at 135.42 ppm. At 146.41 ppm there is a signal of an impurity in the reactants found in every spectrum. Hydrolysis products of 2-chloro-4,4,5,5-tetramethyl-1,3,2-dioxaphospholane could be detected at 175.27 ppm (2-chloro-4,4,5,5-tetramethyl-1,3,2-dioxaphospholane), 132.17 ppm (hydrolysis products of 2-chloro-4,4,5,5-tetramethyl-1,3,2-dioxaphospholane (2,2'-oxybis[4,4,5,5-tetramethyl-1,3,2-dioxaphospholane])), 16.87-16.47 ppm (hydrolysis products of 2-chloro-4,4,5,5-tetramethyl-1,3,2-dioxaphospholane (1,3,2-dioxaphospholane, 4,4,5,5-tetramethyl-, 2-oxide))

Photo-DSC measurements

Sample sizes of approximately 12 mg were weighed into aluminium crucibles, which were subsequently covered with a glass lid. DSC was measured with a DSC 204 F1 Phoenix device from Netzsch with an autosampler and a double-core glass-fiber light guide with a diameter of 3 mm. An empty crucible was measured as the reference. The light source was either an Omnicure lamp with a wavelength of 320 – 500 nm (irradiation time 2 x 300 s, 70 mW cm⁻² at the samples surface) or an LED with a wavelength of 385 nm (irradiation time 2 x 300 s, 70 mW cm⁻² at the samples surface), both at 70 °C. The conversion (C, %) was calculated using **Equation 1**, where H_p is the experimentally determined heat of polymerization (J g⁻¹), $H_{o,p(i)}$ is the theoretical heat of polymerization for compound i (J mol⁻¹; 100 kJ mol⁻¹ for epoxy alcohols [19a] and 56 kJ mol⁻¹ for methacrylates [22]), M_i is the molecular weight (g mol⁻¹) and X_i is the molar ratio of compound i . The maximum rate of polymerization ($R_{p,max}$, s⁻¹) was calculated using **Equation 2**, where h is the experimentally determined maximum peak height (J g⁻¹), M is the molecular weight (g mol⁻¹), n is the number of reactive groups per molecule, and $\Delta H_{o,p}$ is the difference between the values for the theoretical heat of polymerization indicated above. [21]

$$\text{Conversion} = \left[\frac{H_p}{\sum \frac{H_{o,p(i)} \cdot X_i}{M_i}} \right] * 100 \quad [1]$$

$$R_{p,max} = \frac{hM}{n\Delta H_{p,0}} \quad [2]$$

Dynamic mechanic thermal analysis

The samples were cured into 2x5x40 mm³ specimens as described above. The DMTA measurements were conducted on an Anton Paar MCR 301 device with a CTC 450 oven. Torsion mode was applied with a frequency of 1 Hz, a strain of 0.1% and a temperature ramp from 100 to 200 °C with a heating rate of 2 K min⁻¹. Specimens were clamped into the device cautiously. The software RheoCompass V1.24 by Anton Paar was used for data recording and evaluation. The T_g was extracted as the maximum of the $\tan \delta$ curve. G'_{25} was determined as the storage modulus at 25 °C.

3D printing and post processing

A DLP printer with a DLP-light engine that irradiates at 385 nm with a maximum intensity of 75 mW cm⁻² was utilized. The customized printer is optimized for resin development, requiring only small amounts of formulation up to 7.5 mL. Pixel sizes of 50 μ m are projected on an area of 96 mm x 54 mm. The printed parts are built on a building platform of 42 x 38 mm. Since the smallest voxel of the printer is 50 μ m, the lines and dots in the resolution test chip were designed to increase in steps of 50 μ m for every voxel added in the STL file. The printed parts were cleaned by using an airbrush filled with acetone for approximately 60s to remove residual monomer. Submersion in solvent in combination with ultrasonic bath was not possible since it would have dissolved the uncured hard network within the printed part. After cleaning, the printed parts were irradiated in the UV/vis-oven for 300 s per side (Uvitron International INTELLIRAY 600 UV-oven; 320-500 nm Hg broadband UV lamp; 600 W; UV-A: 125 mW cm⁻²; vis: 125 mW cm⁻²). Finally, they were post-cured at 110 °C for approximately 16 h. The double bond conversion was checked via ATR-IR and was found to be 98.2 % \pm 1.1 %.

Microscopic analysis of 3D printed objects

The digital microscope used was a Keyence VHX6000 with an objective with 20-200x zoom. Scanning electron microscopy (SEM) images were obtained from a Zeiss EVO 10 device equipped with an Everhart-Thornley secondary electron detector and SmartSEM software. The sample was sputtered with a thin gold layer for conductivity and placed on a conductive carbon pad. The acceleration voltage was 3 kV.

FT-ATR-IR

The IR-spectra were recorded on a PerkinElmer Spectrum 65 FT-IR Spectrometer equipped with a Specac MKII Golden Gate Single Reflection ATR System. Four scans per measurement in a range of 500 cm⁻¹ to 4000 cm⁻¹ were performed with 11 measurements per sample. Solid samples (cured, c) were pressed onto the ATR-IR crystal with a screw and liquid samples (uncured, u) were applied directly onto the ATR-IR crystal. For evaluation, the reference peak (ref) from 1775 cm⁻¹ to 1650 cm⁻¹ was used (stretching vibration ν (C=O)), for evaluation of double bond peak of the methacrylates (m) the peak from 1647 cm⁻¹ to 1630 cm⁻¹ (stretching vibration ν (C=C)) was used.¹ For calculation of the double bond conversion, the areas of evaluated peaks were divided by the reference peak to yield a relative peak area difference for cured (c) and uncured (u) samples, independent of compressive strength of the sample onto the ATR-IR crystal. The relative peak areas of the cured samples were then referenced to the relative peak area of uncured formulation to obtain the double bond conversion [3].

$$DBC = 1 - \left(\frac{A_{c,m}}{A_{c,ref}} \div \frac{A_{u,m}}{A_{u,ref}} \right) \quad [3]$$

2. Macro-methacrylate analysis

To determine the degree of endgroup functionalization, the unmodified (Figure S6) and modified (Figure S7) polyester's ^{31}P -NMRs were measured to determine the OH-number as described above.

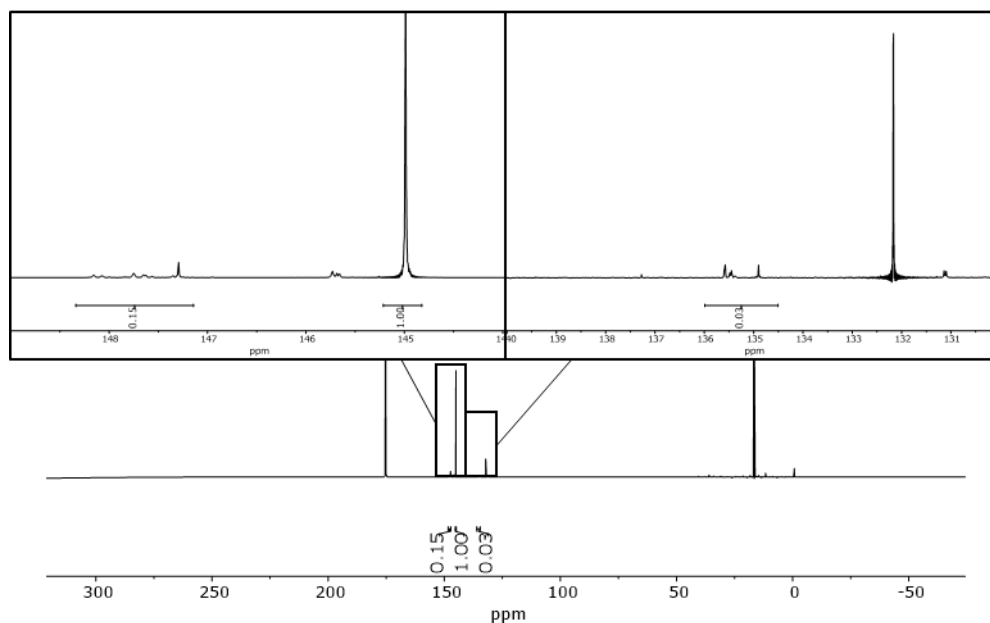


Figure S1: ^{31}P -NMR of the modified polyester (175.27 ppm: 2 chloro-4,4,5,5-tetramethyl-1,3,2-dioxaphospholane, 147.30 ppm: aliphatic OH-groups of unmodified polyester 146.41 ppm: impurity in the reactants found in every spectrum, 144.99 ppm: cyclohexanol, 135.42 ppm: acidic OH-groups of unmodified polyester 132.17 ppm: hydrolysis products of 2 chloro-4,4,5,5-tetramethyl-1,3,2-dioxaphospholane (2,2'-oxybis[4,4,5,5-tetrakis(4-methyl-1,3,2-dioxaphospholane)]), 16.87-16.47 ppm: hydrolysis products of 2 chloro-4,4,5,5-tetramethyl-1,3,2-dioxaphospholane (1,3,2-dioxaphospholane, 4,4,5,5-tetramethyl-, 2-oxide)).

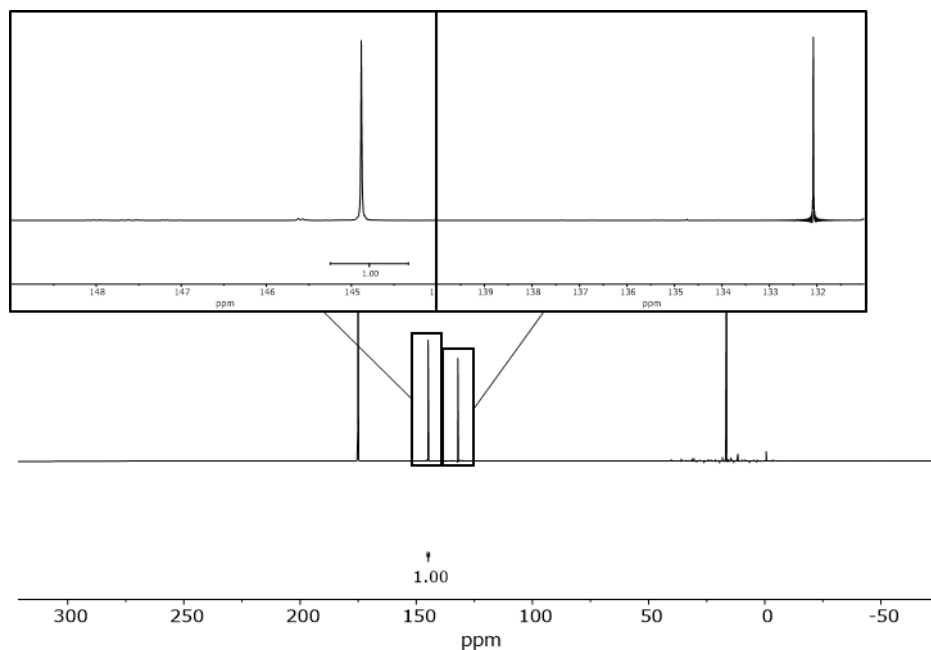
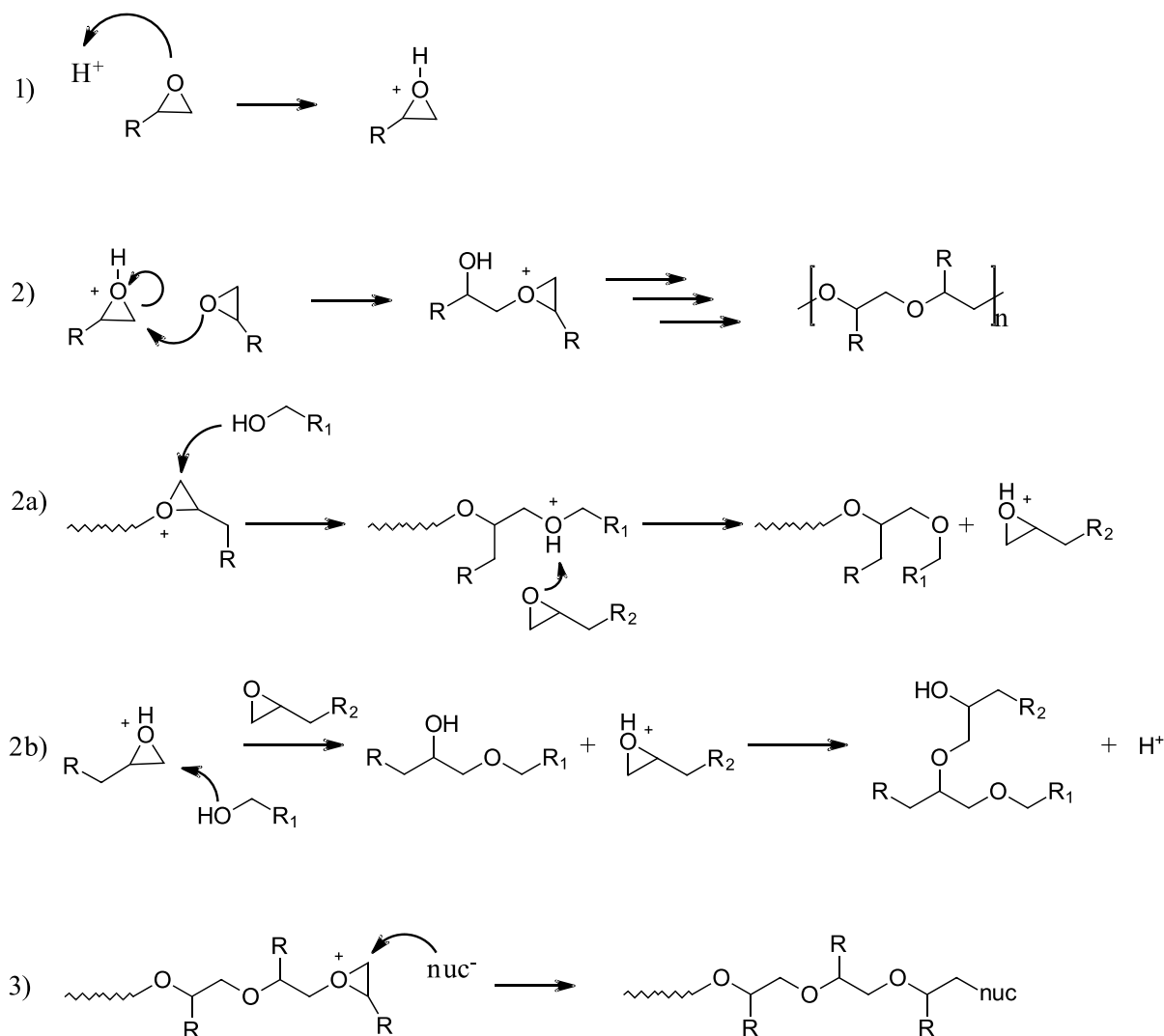


Figure S2: ^{31}P -NMR of the modified polyester (175.27 ppm: 2 chloro-4,4,5,5-tetramethyl-1,3,2-dioxaphospholane, 146.41 ppm: impurity in the reactants found in every spectrum, 144.99 ppm: cyclohexanol, 132.17 ppm: hydrolysis products of 2 chloro-4,4,5,5-tetramethyl-1,3,2-dioxaphospholane (2,2'-oxybis[4,4,5,5-tetrakis(4-methyl-1,3,2-dioxaphospholane)]), 16.87-16.47 ppm: hydrolysis products of 2 chloro-4,4,5,5-tetramethyl-1,3,2-dioxaphospholane (1,3,2-dioxaphospholane, 4,4,5,5-tetramethyl-, 2-oxide)).

3. Chain transfer mechanism for epoxides with alcohols



Scheme S2: Mechanism of cationic polymerization of an epoxide: 1) addition of the acidic hydrogen at the reactive site of the monomer 2) propagation of the chain reaction by the addition of a monomer to the active chain end (ACE mechanism) 2a) chain transfer via an intermolecular mechanism, a mildly nucleophilic compound attacks the electrophilic carbon of the oxirane ring, the acidic H can be abstracted by another monomer and can therefore reinitiate a new polymer chain 2b) active monomer (AM) mechanism, alcohol adds to activated monomer, forms a new alcohol and an acidic hydrogen, which itself can activate another monomer 3) termination of the chain reaction by addition of a nucleophilic compound.^{2,3}

4. Epoxide screening

Four epoxides were screened with and without addition of trimethylolpropane (T) as chain transfer agent for their use in the hard network (Table S1). Mixing them with the alcohol lead to an overall decrease in tensile strength, whilst simultaneously increasing the strain at break and toughness (Figure S3, Table S2). This effect can be attributed to the chain transfer properties of the alcohols. The results suggest that resorcinol diglycidylether was the best suitable epoxide out of all tested epoxides, both before and after addition of multifunctional alcohols for chain transfer (Figure 2, Table S3). The stresses reached at the yield point and at break follow a clear trend, indicating that more rigid epoxide structures increase stress resistance. Therefore, the aromatic epoxide R performed best, followed by the fused ring cycloaliphatic epoxide CE, the floppier cycloaliphatic epoxide DE, and finally the linear aliphatic epoxide TE. It is noteworthy that the effect of epoxide rigidity becomes more pronounced upon introduction of alcohols as chain transfer agents, which decrease the network density. Hence, R was utilized for all consecutive studies.

Table S1: Formulation compositions for the epoxide alcohol system, including functional group equivalents (fg%) of the epoxide resorcinol diglycidyl ether (R) and alcohol (trimethylolpropane (T) or benzyl dimethanol (B)). Polymers of R and T (RT) or R and B (RB) were obtained from formulations containing the compounds in a 1:1 functional group ratio. Formulations were cured analogously with the photoacid generator UVI6979.

	R		ALCOHOL		UVI6976
	[g]	[fg%]	[g]	[fg%]	[g]
RT	2.4931	50	1.0047	50	0.03237
RB	2.1585	50	1.3417	50	0.03477

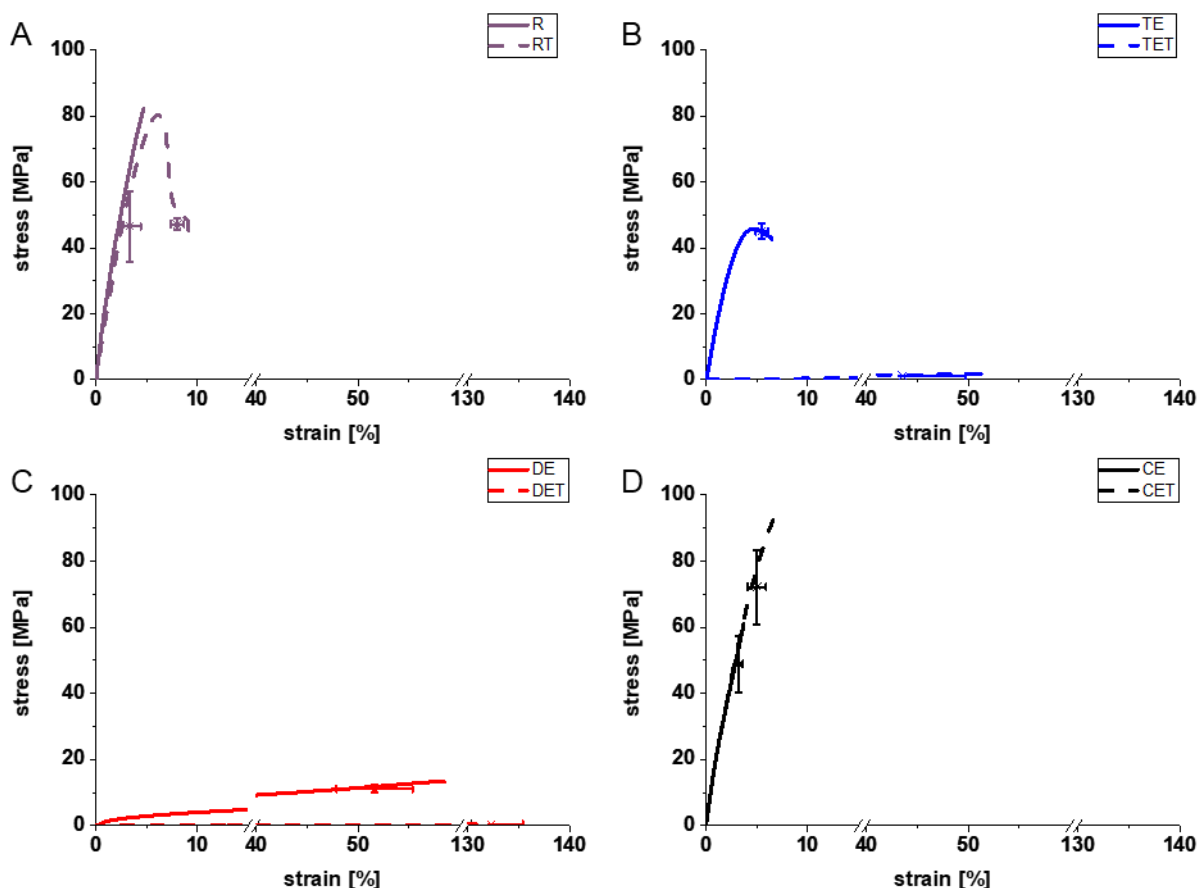


Figure S3: Screening of four epoxides with and without trimethylolpropane (T) as chain transfer agent A) resorcinol di-glycidylether (R).: B) trimethylolpropane triglycidylether (TE), C) cyclohexane dimethanol diglycidylether (DE), D) 3,4-epoxycyclohexylmethyl 3,4-epoxycyclohexanecarboxylate (CE), Mixtures of epoxides with trimethylolpropane contained equimolar amounts of both compounds with respect to their reactive groups.

Table S2: Screening of four epoxides with and without trimethylolpropane (**T**) as chain transfer agent as depicted in Figure S1: 3,4-epoxycyclohexylmethyl 3,4-epoxycyclohexanecarboxylate (**CE**), cyclohexane dimethanol diglycidylether (**DE**), trimethylolpropane triglycidylether (**TE**), Resorcinol diglycidylether (**R**). Mixtures of the respective epoxides with **T** contained equimolar amounts of reactive groups.

		Strain at break	Ultimate Tensile strength	Tensile toughness
		[%]	[MPa]	[MJ m ⁻³]
Epoxide	CE	3.2 ± 0.4	48.9 ± 8.4	0.9 ± 0.2
	DE	51.6 ± 3.7	11.1 ± 1.1	3.4 ± 0.5
	TE	5.5 ± 0.6	45.0 ± 2.3	1.7 ± 0.3
	R	6.5 ± 2.6	46.5 ± 10.6	1.0 ± 0.8
Epoxide + alcohol	CET	5.0 ± 0.9	72.1 ± 11.3	2.1 ± 0.8
	DET	132.3 ± 3.1	0.4 ± 0.1	0.3 ± 0.1
	TET	43.5 ± 6.3	1.2 ± 0.1	0.4 ± 0.1
	RT	8.0 ± 0.7	47.2 ± 1.8	4.1 ± 0.4

Table S3: (Thermo)mechanical data of epoxide and epoxide alcohol systems depicted in Figure 2 (**R**: resorcinol diglycidyl ether, **T**: trimethylolpropane, **B**: benzyl dimethanol, **RT**: polymer of **R** and **T** in a 1:1 functional group ratio, **RB**: polymer of **R** and **B** in a 1:1 functional group ratio).

	Tensile strength	Strain at break	T _g
	[MPa]	[%]	[°C]
R	3.3 ± 1.1	46.5 ± 10.6	110
RT	8.0 ± 0.7	47.2 ± 1.8	59
RB	9.2 ± 2.0	66.8 ± 5.4	72

5. (Thermo)mechanical data of resorcinol diglycidylether-based IPNs with and without alcohols

The following tables summarize relevant formulation compositions (Tables S4-S5) and key results of photo-DSC (Table S6), DMTA, and tensile testing data (Tables S7) of all three IPN formulations (**IPN 25-50 wt%**) compared to the pure epoxide (**R**) and the optimized hard network (**RT**) presented in the main manuscript.

Table S4: Formulation compositions for the IPNs in functional group equivalents (wt%) of the epoxide resorcinol diglycidyl ether (**R**), alcohol (trimethylolpropane (**T**), Homosalte methacrylate (**HSMA**) and the modified polyester (**M**). Polymers of **R** and **T** (**RT**) or **R** and **B** (**RB**) were obtained from formulations containing the compounds in a 1:1 functional group ratio. Formulations were cured analogously with the photoacid generator UVI6979.

	R	T	HSMA	Polyester methacrylate	UVI6976	TPO-L
	[wt%]	[wt%]	[wt%]	[wt%]	[wt%]	[wt%]
IPN 25wt%	54	21	19	6	1	1
IPN 35wt%	46	19	26	9	1	1
IPN 50wt%	36	14	37	13	1	1

Table S5: Formulation compositions for the IPNs as described in Table S3, expressed in grams of alcohol (trimethylolpropane (T), homosalte methacrylate (HSMA), modified polyester (M), and cationic (UVI6976) and radical initiator (TPO-L) weighed in. Polymers of R and T (RT) or R and B (RB) were obtained from formulations containing the compounds in a 1:1 functional group ratio. Formulations were cured analogously with the photoacid generator UVI6979.

	R	T	HSMA	Polyester methacrylate	UVI6976	TPO-L
	[g]	[g]	[g]	[g]	[g]	[g]
IPN 25wt%	2.7197	1.0784	0.9384	0.3181	0.0558	0.05129
IPN 35wt%	2.3235	0.944	1.3143	0.4374	0.05522	0.05152
IPN 50wt%	1.8032	0.7161	1.8835	0.629	0.05248	0.05034

Table S6: Photo-DSC data depicted in Figure 3 (R: resorcinol diglycidyl ether, T: trimethylol propane, RT: polymer of R and T in a 1:1 functional group ratio, IPN X wt%: polymer consisting of X wt% methacrylate network (75 wt% for homosalte methacrylate, 25 wt% of the modified polyester) and 100-X wt% RT

	t _{onset} [s]	t _{max} [s]	t _{95%} [s]
RT	12.0± 1.5	26.9± 1.2	117.3± 12.2
IPN 25wt%	5.7± 0.1	11.1± 0.1	34.7±2.5
IPN 35wt%	6.0± 0.1	11.7±1.3	38.4±2.3
IPN 50 wt%	5.8± 0.1	11.0±0.1	36.1±1.8

Table S7: (Thermo-)mechanical data of IPN-T depicted in Figure 4 (R: resorcinol diglycidyl ether, T: trimethylol propane, RT: polymer of R and T in a 1:1 functional group ratio, IPN X wt%: polymer consisting of X wt% methacrylate network (75 wt% for homosalte methacrylate, 25 wt% of the modified polyester) and 100-X wt% RT

	Strain at break	Ultimate Tensile strength	Tensile toughness	T _g
	[%]	[MPa]	[MJ m ⁻³]	[°C]
R	3.03± 1.1	46.5± 10.6	0.97± 0.76	110
RT	8.0± 0.7	47.2± 1.8	4.14± 0.41	59
IPN 25wt%	2.6±0.7	42.36±6.7	0.6±0.3	65
IPN 35wt%	17.03± 0.7	38.4± 7.9	7.20±3.14	53
IPN 50wt%	14.0±5.0	18.5±1.4	2.2±0.7	73

6. Photo-DSC results

The methacrylate network formation in presence of the epoxide monomers and alcohol chain transfer agents was observed by means of photo-DSC, omitting the photoacid generator in IPN formulations to prevent co-curing of the epoxy network (Figure S4).

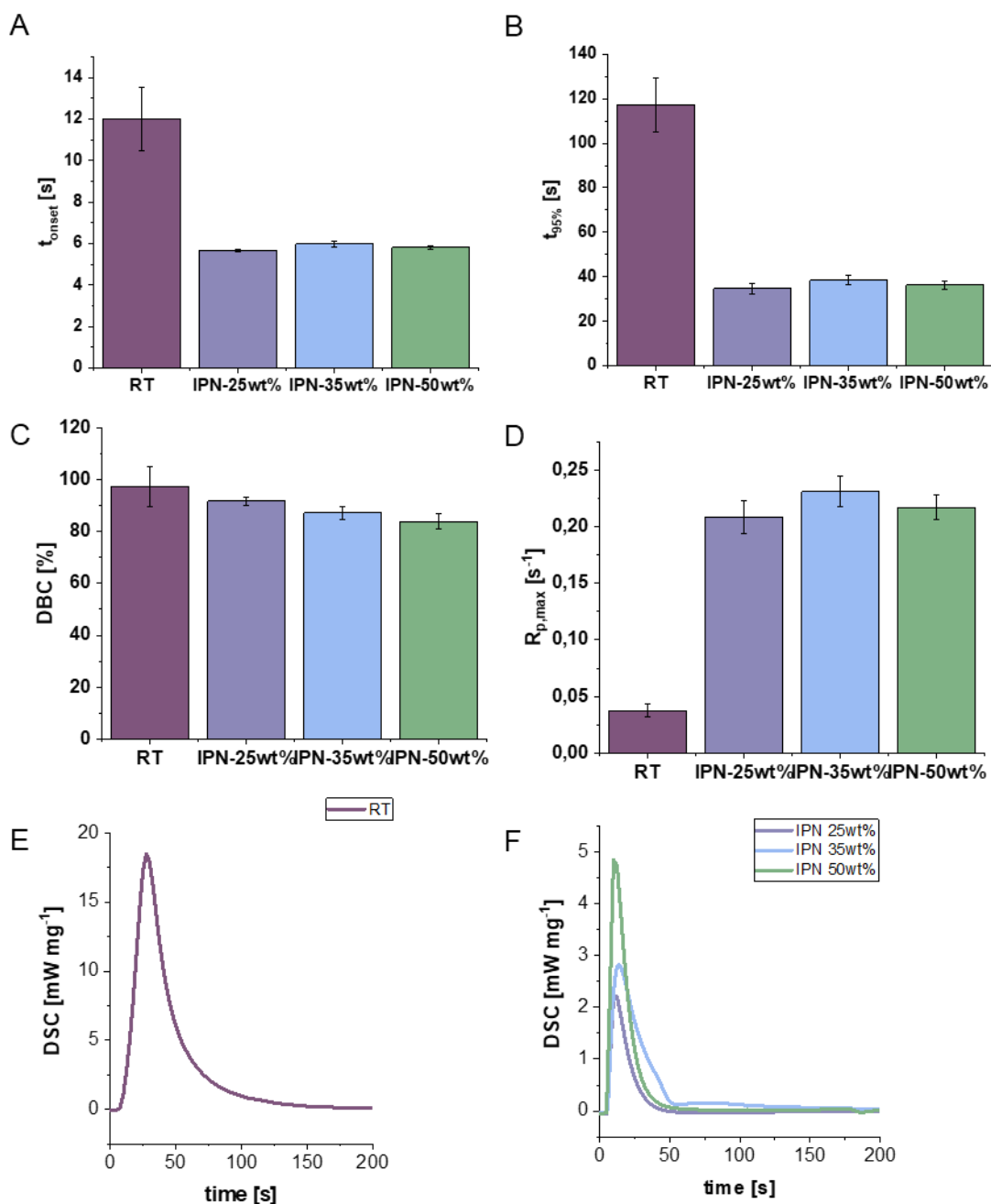


Figure S4: Reactivity characteristics of only the methacrylate-reactivity in the IPN formulation, i.e. in appropriate dilution with the epoxide system obtained from photo-DSC measurements in the presence of the radical initiator and in the absence of the photoacid generator. A) Time until the onset of heat evolution (t_{onset}), B) time until 95% of heat evolution is reached ($t_{95\%}$), C) double bond conversion (DBC; epoxy group conversion for RT; calculated according to the procedure in the Experimental section), and D) rate of polymerisation ($R_{p,max}$) for varying methacrylate resin concentrations in the IPN E) Curve of RT F) Photo-DSC curve of IPN 25wt%, IPN 35wt%, IPN 50wt% (IPN-X: 100-X wt% hard network consisting of resorcinol diglycidylether and trimethylolpropane (RT) + X wt% methacrylate network consisting of 75 wt% for homosalate methacrylate and 25 wt% for the modified polyester).

Furthermore, the photo-DSC experiment was performed with an LED light source centered around 385 nm to demonstrate the semi-orthogonal curing behaviour of IPN 35 wt% in comparison to RT alone under the printing conditions (**Figure S3**). For this purpose, the IPN 35 wt% formulation and the formulation for the hard network alone, consisting of resorcinol diglycidylether and trimethylolpropane (**RT**), were both irradiated in the DSC and heat evolution was measured. As expected, **RT** does not react under these conditions. The results of the photo-DSC measurements can therefore be attributed to the radical system.

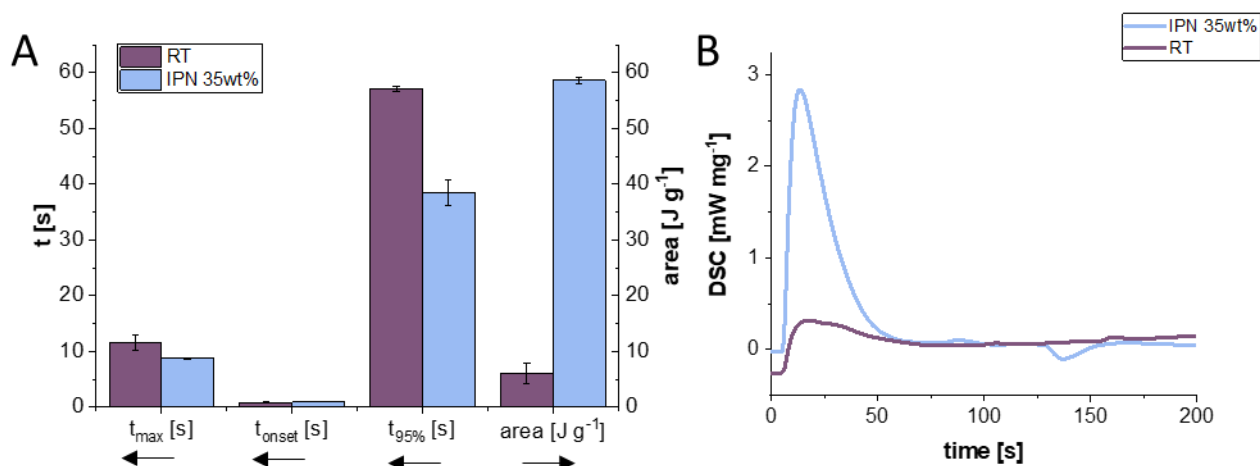


Figure S5: A) Photo-DSC measurements of RT and IPN-T 35wt% with LED light source (300 s irradiation time, 385 nm, 70 mW cm⁻²) B) curves of the measurements.

7. DMTA results

DMTA measurements were performed to investigate the (thermo-) mechanical properties of the cured IPNs, most importantly its glass transition. Thereby, the loss factor (Figure 4) is the ratio of the loss (G'') and storage (G') modulus (Figure S6), indicating the relative degree of energy dissipation or damping of the material.

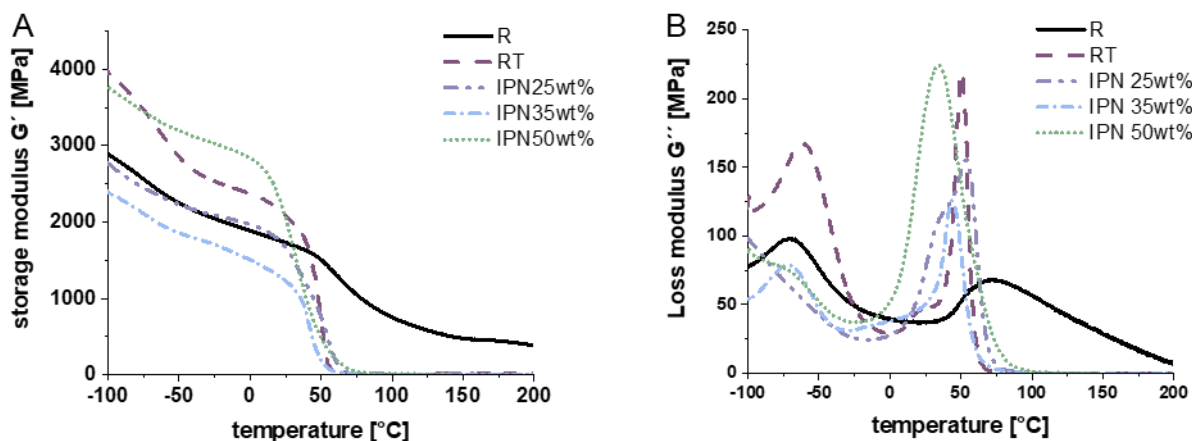



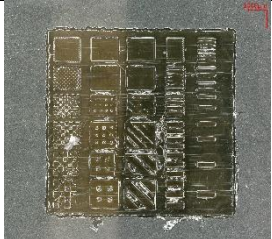
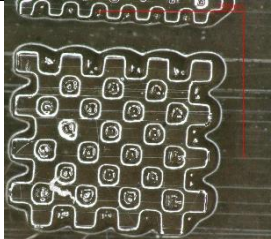
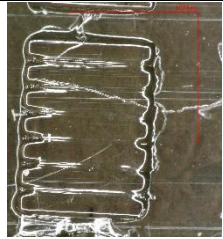

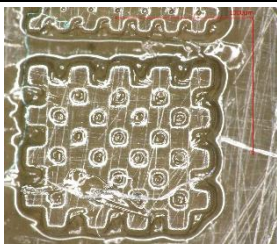
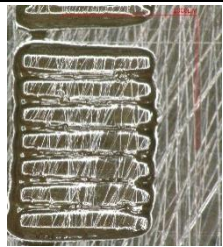
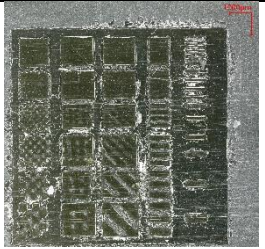

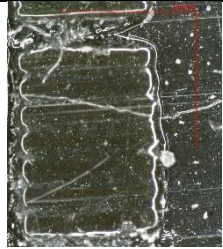
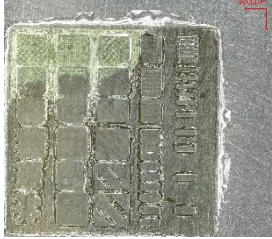
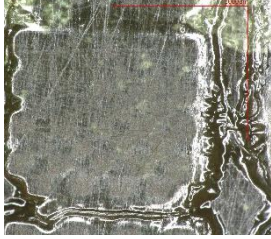



Figure S6: A) storage modulus and B) loss modulus of the cured epoxy(-alcohol) systems and the IPNs IPN 25wt%, IPN 35wt%, IPN 50wt% (IPN-X: 100-X wt% hard network consisting of resorcinol diglycidylether and trimethylolpropane (RT) + X wt% methacrylate network consisting of 75 wt% for homosalate methacrylate and 25 wt% for the modified polyester).

8. 3D printing of RT

To determine under which irradiation times and intensities the pure hard network could be cured, resolution test chips were printed at the highest intensity of the printer for varying irradiation times (Table S7).

Table S8: Resolution tests for printing of the hard network containing resorcinol diglycidyl ether and trimethylolpropane (RT) with different irradiation times at 75 mW cm^{-2} : complete printed chip (1st column), grid of 2x2 voxel size ($100 \mu\text{m}$; 2nd column), and lines with a width of $100 \mu\text{m}$ (3rd column).

Irradiation time	Full	Grid	Lines
30 s			
32.5 s			
35 s			
37.5 s			
40 s			

9. 3D printing of IPN 35 wt%

Printing tests of IPN 35 wt% were successful, although the yielded gels were too soft for complex structures and were partially destroyed while removing them from the platform.

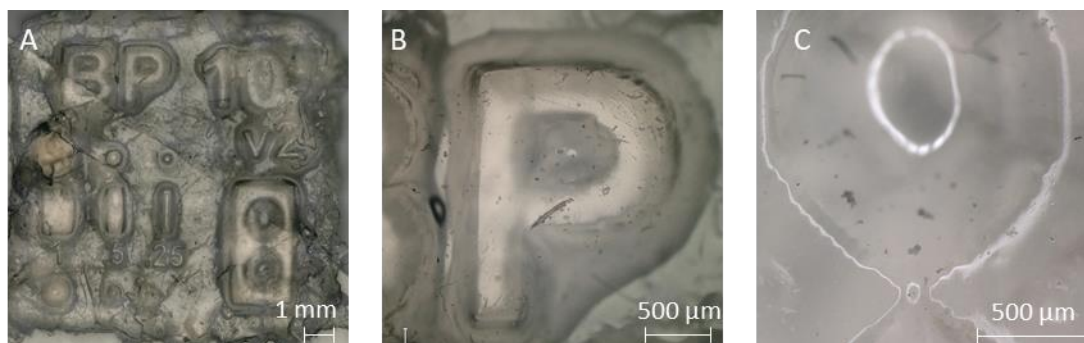
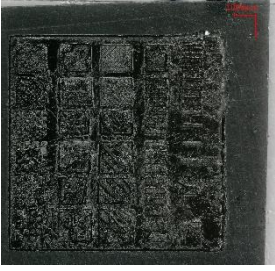
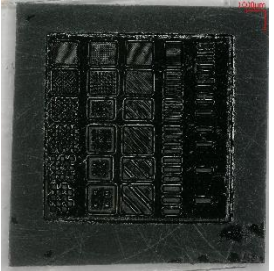
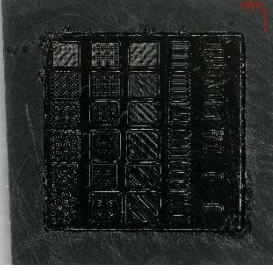


Figure S7: Printed parts from IPN 35 wt%: A) whole chip, B) zoom on P, C) zoom on hour glass

10. 3D printing of IPN 50 wt%

The light intensity for 3D printing of the IPN 50 wt% formulation was optimized utilizing a resolution test grid (Table S6).

Table S9: Resolution tests for printing of IPN 50wt% with different irradiation times and different light intensities (sample 3s 20 mW cm⁻² got disrupted during cleaning)

Irradiation time	3s	6s	8s
Light intensity	20 mW cm ⁻²	10 mW cm ⁻²	7.5 mW cm ⁻²
Outcome			

Under the optimized conditions, a variety of objects was printed (Figure S9).

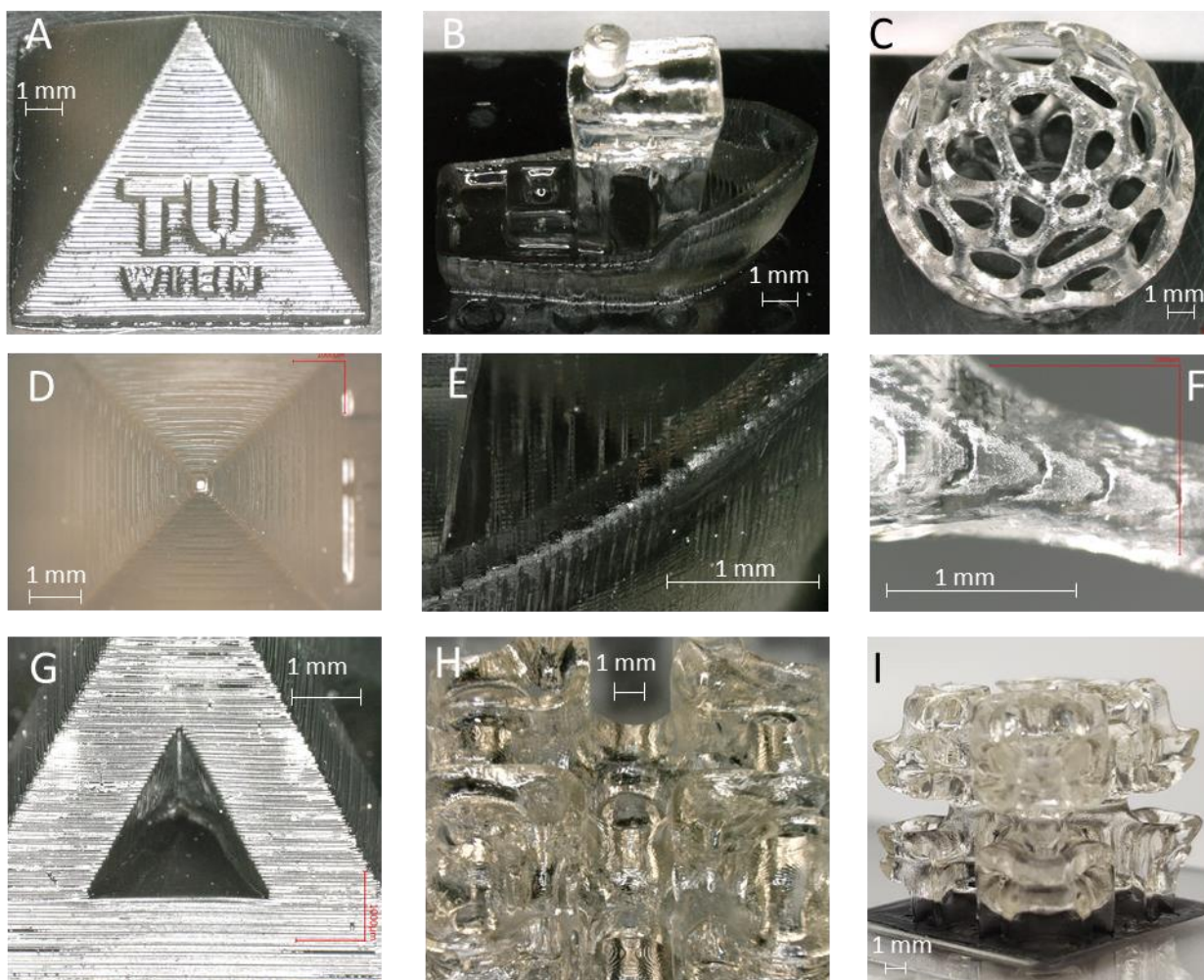


Figure S8: Printed parts from IPN 50 wt%: A) solid pyramid with TU Wien inscription front view, B) Benchy side view, C) hollow ball front view, D) solid pyramid with TU Wien inscription top view, E) zoomed-in view of Benchy, F) zoomed-in view of the hollow ball, G) hollow pyramid front view, H) complex structure front view, I) complex structure side view.

11. References

1. P. Carion, A. Ibrahim, X. Allonas, C. Croutxé-Barghorn and G. L'Hostis, *Journal of Polymer Science Part A: Polymer Chemistry*, 2019, **57**, 898-906.
2. S. Aoshima and S. Kanaoka, *Chemical Reviews*, 2009, **109**, 5245-5287.
3. B. Dillman and J. L. P. Jessop, *J Polym Sci Pol Chem*, 2013, **51**, 2058-2067.